DOI: 10.1534/genetics.110.125906

Modifier Genes for Mouse Phosphatidylinositol Transfer Protein α (*vibrator*) That Bypass Juvenile Lethality

Dorothy Concepcion,* Frank Johannes,† Yuan Hung Lo,* Jay Yao,* Jerry Fong*,[1] and Bruce A. Hamilton*,[2]

**Department of Medicine, Department of Cellular and Molecular Medicine, and Institute for Genomic Medicine, University of California San Diego, La Jolla, California 92093-0644 and †Groningen Bioinformatics Centre, University of Groningen, 9751NN Haren, The Netherlands*

Manuscript received December 13, 2010
Accepted for publication February 10, 2011

ABSTRACT

Phosphatidylinositol transfer proteins (PITPs) mediate lipid signaling and membrane trafficking in eukaryotic cells. Loss-of-function mutations of the gene encoding PITPα in mice result in a range of dosage-sensitive phenotypes, including neurological dysfunction, neurodegeneration, and premature death. We have previously reported genetic suppression of a strong hypomorphic allele, *vibrator*, by a wild-derived variant of *Nxf1*, which increases the level of PITPα made from *vibrator* alleles and suppresses each of the neurological and survival phenotypes. Here we report discovery and genetic mapping of additional *vibrator* modifiers, *Mvb2* and *Mvb3*, from a different strain background that suppresses juvenile lethality without suppressing visible phenotypes or gene expression. Genotype-specific survival analysis predicts molecular heterosis at *Mvb3*. These results indicate a mechanism of suppression that bypasses a quantitative requirement for PITPα function.

PHOSPHATIDYLINOSITOL transfer proteins (PITPs) are defined by the ability to transfer phosphatidylinositol (PI) between membranes (McMurray and Dawson 1969; Helmkamp *et al.* 1974). This activity is found in all eukaryotic cells examined and is essential for sustained lipid signaling, intracellular trafficking, and other membrane transactions (Phillips *et al.* 2006b; Cockcroft and Carvou 2007). Functional PITPs include small soluble proteins, represented by PITPα and PITPβ in mammals (class I); a homologous subfamily of larger, membrane-spanning proteins typified by the Drosophila *retinal-degeneration B* (RdgB) protein (class II); and a nonhomologous group related to yeast Sec14p (class III). Despite a high level of sequence identity between PITPα and PITPβ, the proteins have different subcellular distributions, with PITPα distributed throughout the cytoplasm and PITPβ concentrated at the Golgi complex (De Vries *et al.* 1995; Phillips *et al.* 2006a). Each of the known PITP proteins can catalyze transfer of distinct groups of related lipids, typically including inositol-phosphorylated derivatives of PI and lipids with other head groups, such as phosphatidylcholine. PITPs also present lipids to localized compartments or signaling "nanoreactors," which may provide a logic to the existence of integral membrane forms and some of the genetic properties of soluble PITPs (Ile *et al.* 2006).

The first class I PITP mutation was identified by positional cloning of the mouse juvenile neurodegeneration mutant, *vibrator* (*vb*). This hypomorphic allele, caused by a retrovirus insertion into an intron, has an ~80% reduction in *Pitpna* RNA and PITPα protein (Hamilton *et al.* 1997). Homozygotes have a progressive action tremor, degenerative pathology in brainstem and spinal cord neurons, and die before sexual maturity on most genetic backgrounds (Weimar *et al.* 1982; Hamilton *et al.* 1997; Floyd *et al.* 2003). Subsequent analysis of a null allele revealed both more severe neurological deficits and a peripheral requirement for PITPα activity for dietary lipid uptake and tissue ATP levels (Alb *et al.* 2003). Metabolic defects seen in these knockout mice are not found in *vibrator* animals on the same genetic background, indicating that PITPα level rather than genetic background is the primary determinant of these peripheral and metabolic phenotypes (Alb *et al.* 2007).

Genetic experiments with *vibrator* have identified strain backgrounds that extend survival (Weimar *et al.* 1982; Hamilton *et al.* 1997; Floyd *et al.* 2003). Weimar *et al.* (1982) originally showed extended survival on a BALB/cBy background, despite persistent neuropathology, but the mechanism and genetic basis remain un-

Supporting information is available online at http://www.genetics.org/cgi/content/full/genetics.110.125906/DC1.

[1]*Present address:* Huffington Center on Aging, 1 Baylor Plaza, Baylor College of Medicine, Houston, TX 77030.

[2]*Corresponding author:* George Palade Laboratories for Cellular and Molecular Medicine, UCSD School of Medicine, 9500 Gilman Dr., La Jolla, CA 92093-0644. E-mail: bah@ucsd.edu

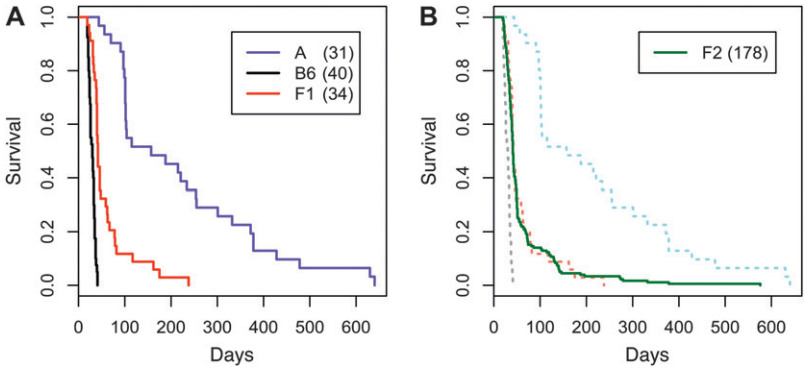

FIGURE 1.—A/J background extends the life span of *vb/vb* animals. (A) Kaplan–Meier plot shows survival at indicated ages for contemporaneous cohorts of A/J(N3F1)–*vb/vb*, B6–*vb/vb*, and AxB(F1)–*vb/vb* animals. Differences between groups are significant for each comparison ($P < 10^{-6}$ by both the log rank test and a Cox proportional hazards model). (B) Survival of AxB(F2)–*vb/vb* animals drawn from two independent cohorts approximates the F_1 cohort shown in A. Beginning cohort sizes are indicated in parentheses.

explored. We described a CAST/Ei-derived locus on chromosome 19, initially designated *Mvb1*. Positional complementation cloning identified *Mvb1* with a wild-derived *Mus musculus castaneus* allele of the nuclear export factor *Nxf1* (FLOYD *et al.* 2003). Subsequent experiments show that this modifier suppresses mutations caused by intracisternal A particle endogenous retroviruses inserted into introns as a class, in each case by increasing the level of correctly spliced mRNA derived from the inserted allele (CONCEPCION *et al.* 2009). In the case of *vibrator*, the increased RNA and protein level is sufficient to attenuate tremor and neurodegeneration phenotypes substantially and to eliminate most premature lethality (HAMILTON *et al.* 1997; FLOYD *et al.* 2003). As mutations in other components of PI signaling pathways have an overlapping range of neurological and cellular phenotypes (NYSTUEN *et al.* 2001; CHOW *et al.* 2007; ZHANG *et al.* 2007; JIN *et al.* 2008), identification of modulatory pathways for one may have broader importance for related mouse models and human disorders.

Here we demonstrate genetic suppression of *vibrator* lethality, independent of other phenotypes, in A/J mice. In contrast to *Mvb1*, this suppression does not alter the gross distribution of neuropathology and does not notably alter the *Pitpn* expression level. We identify QTL for survival of *vibrator* animals by recombination mapping, using both a standard nonparametric model to detect QTL with broad effect and a recently developed time-dependent model to detect QTL with time-specific effects on survival.

MATERIALS AND METHODS

Mice and genotyping: All animals were bred in an Association for Assessment and Accreditation of Laboratory Animal Care (AAALAC)-accredited vivarium in accordance with protocols approved by the University of California San Diego Institutional Animal Care and Use Committee. Animals were maintained on 12-hr light/dark cycles and with ad libitum access to food and water. Congenic B6–*vb* stock has been described (FLOYD *et al.* 2003; CONCEPCION *et al.* 2009). B6×129–*Gnaq* stock was the gift of Stefan Offermanns and Melvin I. Simon (OFFERMANNS *et al.* 1997a,b). All other lines were obtained from the Jackson Laboratory, Bar Harbor, Maine. Standard histology was performed after staining with hematoxylin and eosin. Genotyping primers for *vb* were wt_for (GTGATCGGGACTTTTGTTTCC), vb_for (AACGCGTCTAA TAACACTTGTG), and both_rev (ACCAAAAGGACTGCCAG TCAT). Genotyping primers for *Gnaq* were GqIN5A (AGGGC CCATGAGGACATGTA), GqNEO (CAAAGTATCACACTCA CATCACAG), and GqTW36 (AGGATCTCGTCGTGACCCAT).

Molecular biology: Reverse transcription-quantitative PCR (RT-qPCR) using SYBR green fluorescence and Western blotting with infrared image quantification were performed using standard methods, adapted as described (CONCEPCION *et al.* 2009). Primers for *Pitpna* were ACACGAGAAAGCCTG GAATG and GTTTATGCACATTCTCCTGG and for *Ppig* (cyclophilin), GGGACAGGGAAATCAACTCA and CCTCCTCTTCCA TTCCCTTC.

Genetic mapping: Microsatellite (SSLP) markers were taken from the Massachusetts Institute of Technology mouse map (DIETRICH *et al.* 1996), available at http://www.informatics.jax.org/ and http://genome.ucsc.edu/. Development of additional markers, to distinguish A and B6 alleles in a long segment of low divergence on chromosome 10, was guided by segments containing SNP polymorphisms in published maps (PLETCHER *et al.* 2004). Informative markers in this interval were D10Bah3 (AGGCTCAAGCTTTTGGCTTA and ACGGCCATGACAGGA AGA) and D10Bah6 (ATCCCTGGGGAAATCTGCT and TGA ATGGGCTTTGGCTGA). Two animals were genotyped twice with each marker, and several markers were typed twice independently as quality assurance on the overall data set.

Data analysis: Mapping tools within R/QTL (BROMAN *et al.* 2003) were used to identify potential genotyping errors. Reexamination and/or replication of initial typing data were used to resolve likely errors. Linkage analysis for survival beyond 42 days as a dichotomous trait was carried out in R/QTL using a nonparametric statistic derived from the Kruskal–Wallace test (BROMAN *et al.* 2003; BROMAN and SEN 2009). Linkage analysis for QTL with time dependence was carried out using an enhanced Cox proportional hazard model (EC) as described (JOHANNES 2007). ANOVA and post-hoc Tukey's honest significant difference (HSD) test were performed in R (v. 2.8.1).

RESULTS

A/J strain background selectively extends *vibrator* survival: We have examined *vibrator* mice on several genetic backgrounds with sufficient power to detect potential modifier genes. F_2 from a BALB/cJ × B6C3–*vb* cross survived to a maximum 67 days. This suggests one or more modifier loci with suppressing alleles in BALB/cJ, but with a modest aggregate effect size. In an attempt to identify genetic interactions between $Pitpn^{vb}$ and a

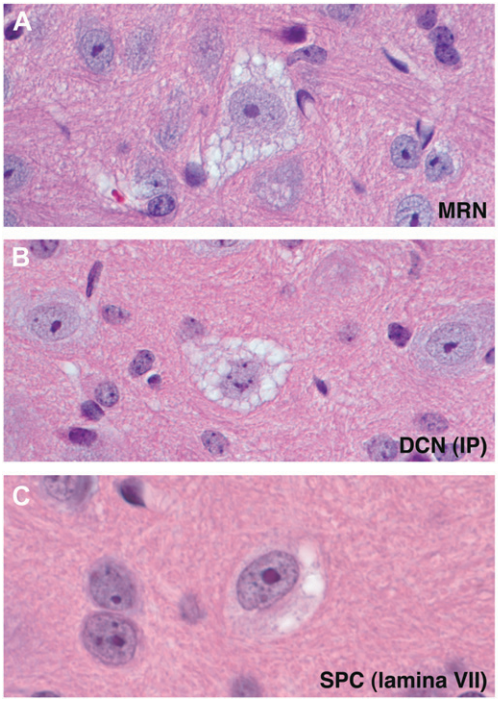

D

	Structure	A–*vb*	B–*vb*
Fore.	Cortex	-	-
	Hippocampus	-	-
Midbrain	Inferior colliculus	+	+
	Midbrain reticular nucleus	+	+
	Red nucleus	++	++
	Substantia nigra	-	-
Hindbrain	Deep cerebellar nuclei (FN, IP, DN)	++	++
	Cerebellar cortex	-	-
	Lateral vestibular nucleus	++	++
	Medial vestibular nucleus	+	+
	Facial motor nucleus	-	-
	Pontine grey	±	±
	Pontine reticular nuclei	++	++
	Gigantocellular reticular nucleus	++	++
	Inferior olivary complex	±	±
Spinal	Dorsal horn	-	-
	Medial laminae	++	++
	Ventral motor neurons	±	-

++ high frequency of cell pathoogy in most animals
+ consistent pathology in most animals
± occasional definite or frequent borderline pathology
- no pathology observed

FIGURE 2.—Neuropathology of *vibrator* is similar in A/J and C57BL/6J backgrounds. Representative vacuolated cells from (A) midbrain reticular nucleus (MRN), (B) interpositus nucleus of the cerebellum [DCN (IP)], and (C) lamina VII of lumbar spinal cord [SPC (lamina VII)]. (D) Comparison of the distribution and relative frequency of pathological changes seen in *vibrator* animals at 28–30 days between the long-surviving A/J and short-surviving B6 backgrounds.

PI-dependent signaling pathway, we also analyzed a cross of B6–*vb* × B6.129–*Gnaq*^{tm1Soff} in considering the hypothesis that decreased signaling through the Gq pathway might attenuate *vb* deficits. Among F_2 progeny, several clearly affected *vb/vb* animals survived several months, while in our congenic B6–*vb* line homozygous animals die within 42 days of birth. However, this prolonged survival effect did not include *Gnaq* mutant animals (indeed, we observed no non-additive interaction between the mutations). The 129-derived cell line that contributed to the *Gnaq* stock is thought to be most closely related to 129S1/SvImJ. Among 79 B6–*vb* × 129S1 F_2 *vibrators*, however, none survived beyond 45 days (supporting information, Figure S1).

In contrast, *vb/vb* progeny in an incipient congenic stock (N3F1) on strain A/J frequently survived beyond 42 days, including some beyond 1 year (Figure 1). To explore this further, we performed survival analysis on B6–*vb*, B6–*vb* × A/J F_2, A/J–*vb* incipient congenic, and B6–*vb* × A/J–*vb* F_1 mutant animals (Figure 1). Cox proportionate hazard models show substantial increases in each group compared with B6–*vb/vb* ($P \sim 10^{-5}$–10^{-12}). Intermediate phenotype of the F_1 group suggests that the effect in aggregate is semidominant. Despite overlapping distributions (Figure 1B), the variance of the F_2 (0.25) is nearly three times that of the F_1 (0.087) due to differences in both tails ($P = 0.02$, *F*-test).

A/J–*vb* retains tremor and neuropathology: Characteristic tremor phenotypes do not appear to be different between *vibrator* animals on A/J and *vibrator* animals on more lethal genetic backgrounds (File S1). We next asked whether the A/J background altered the distribution of cellular neuropathology associated with *vibrator* (Figure 2). Examination of A/J–*vb/vb* animals at P28-30, the same ages reported for B6C3–*vb/vb* (HAMILTON *et al.* 1997) and B6–*vb/vb* (FLOYD *et al.* 2003), showed degenerative changes similar in degree and pattern to those on other backgrounds. Degenerative changes, especially vacuolated cells and faint-staining cells in stages of chromatolysis (HAMILTON *et al.* 1997), were especially frequent in all three deep cerebellar nuclei, in vestibular and reticular nuclei of the hindbrain, and in medial laminae (VI and VII) of the spinal cord (Figure 2, A–C, and Figure S2). In addition, two of five A/J animals examined showed pathology in a single ventral motor neuron among sections through several levels of spinal cord. Vacuolated cells in the midbrain reticular nucleus, inferior colliculus, and superior colliculus were infrequent, but were observed in several *vibrator* animals of both A/J and B6 backgrounds. In both strains, pathology in the red nucleus more frequently appears as faint staining rather than vacuolated cells. As previously reported for other strain backgrounds, A/J–*vb/vb* animals showed no degenerative changes in forebrain, cerebellar cortex, and certain hindbrain nuclei. In all, the pattern of degenerative changes is remarkably similar between A/J–*vb/vb* and B6–*vb/vb* (Figure 2D).

A/J-mediated *vb* suppression does not elevate PITPα expression level: Because the known modifier of *vibrator* acts by elevating the level of *Pitpn* expression from the *vb* allele (FLOYD *et al.* 2003), we asked whether modifiers in A/J might act through a similar mechanism (Figure 3). RT-qPCR analysis of *Pitpn* RNA levels in brain shows that expression in A/J–*vb/vb* is comparable to B6–*vb/vb* and significantly reduced in comparison to B6.CAST–*vb/vb* *Mvb1*^{CAST}/*Mvb1*^{CAST} (Figure 3A) Simi-

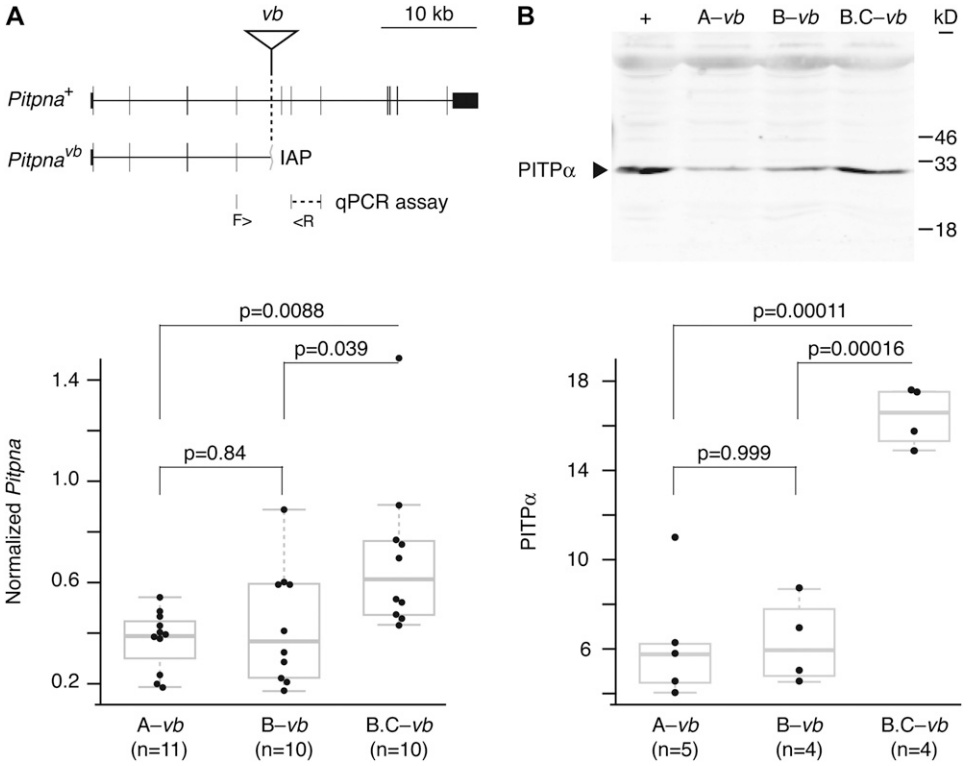

FIGURE 3.—*Pitpn* expression level in A–*vb* is indistinct in B–*vb*. (A) Schematic shows *Pitpna* genomic organization, exon content of normal and mutant transcripts, and design of a selective PCR assay for transcripts that are correctly spliced across the *vb* insertion site in intron 4. Plot shows results from quantitative RT-PCR on brain RNA from *vibrator* mice in congenic A/J (A–*vb*), C57BL/6J (B–*vb*), or B6.CAST–*Mvb1* (B.C–vb) backgrounds. Solid circles represent the average of three triplicate measurements, normalized to cyclophilin (*Ppig*). A–*vb* and B–*vb* show similar levels, and both are significantly less than B.C–*vb*. (B) Western blot showing infrared detection of PITPα. Plot showing quantification of PITPα levels relative to loaded protein are for each individual sample size. Box-and-whisker plots indicate median, quartile, and 1.5 times interquartile range for each class. Indicated *P*-values are from Tukey's HSD test after one-factor ANOVA.

larly, Western blots of PITPα protein in brain show no difference between A/J–*vb/vb* and B6–*vb/vb*, but do detect significantly higher PITPα in *Nxf1*-modified B6.CAST–*vb/vb* $Mvb1^{CAST}/Mvb1^{CAST}$ (Figure 3B).

Linkage analysis identifies A/J modifiers of *vibrator*: To identify major effect modifier loci, we undertook linkage analysis of B6–*vb* × A/J F_2 *vb/vb* animals using survival beyond 42 days (the maximum survival observed among B6–*vb/vb* animals) as a dichotomous trait and using survival latency in days as a quantitative trait (Figure 4). Animals were drawn from two equivalent but independent crosses performed in 2003–2004 (81 *vb/vb*) and 2007–2008 (140 *vb/vb*), with similar phenotype distributions (Kolmogorov–Smirnov test, $P = 0.24$). We genotyped 45 long-lived (≥49 days) and 42 short-lived (≤41 days) animals biased for extreme survival times and including all of the longest-lived (Figure S3 and File S2). Loci on chromosomes 3 and 10 reached genome-wide significance (Figure 4A). The locus on chromosome 3 was significant only for the dichotomous trait of survival past 42 days, while a locus (or possibly two loci) on distal chromosome 10 was significant under both the dichotomous model and the extended Cox model and nearly significant under the normal model (Figure 4B). In addition, loci on chromosomes 4 and 5 showed suggestive linkage, with two loci on chromosome 5 approaching significance under each model tested. X-linked loci did not reach the suggestive threshold for either normal or dichotomous traits and was not tested for the extended Cox model. A two-dimensional scan of the full data set to identify epistatic interactions (BROMAN and SEN 2009) found no significant interactions under either normal or dichotomous models, compared with 1000 permutations of the data. We refer to the locus on chromosome 10 as *Mvb2* and that on chromosome 3 as *Mvb3*.

Genotype-specific distributions of survival periods suggest dominance relationships for each linkage peak (Figure 5). Each locus with at least suggestive genome-wide significance showed allelic effects in the predicted direction, A>B, except the locus on chromosome 4, which is both the weakest and the most model-dependent of the five loci considered. Chromosome 10, the most significant and model-independent linkage peak, shows a semidominant survival effect with AA>AB>BB genotypes. Surprisingly, the significant peak on chromosome 3 shows molecular heterosis with AB>AA or BB. The combination of these two loci is consistent with the overall semidominant effect predicted by comparisons among incipient congenic, F_1, and F_2 animals shown in Figure 1.

DISCUSSION

Phosphatidylinositol transfer proteins function at the intersection of lipid signaling, metabolism, and membrane trafficking. Mutations that dysregulate these activities in animals often manifest as neurological disorders, such as the PITPα-deficient *vibrator* mouse. Modifier genes that mitigate the effects of mutations at one point in this physiological network may show activity toward other components as well, especially if the mechanism of suppression includes bypass of a physio-

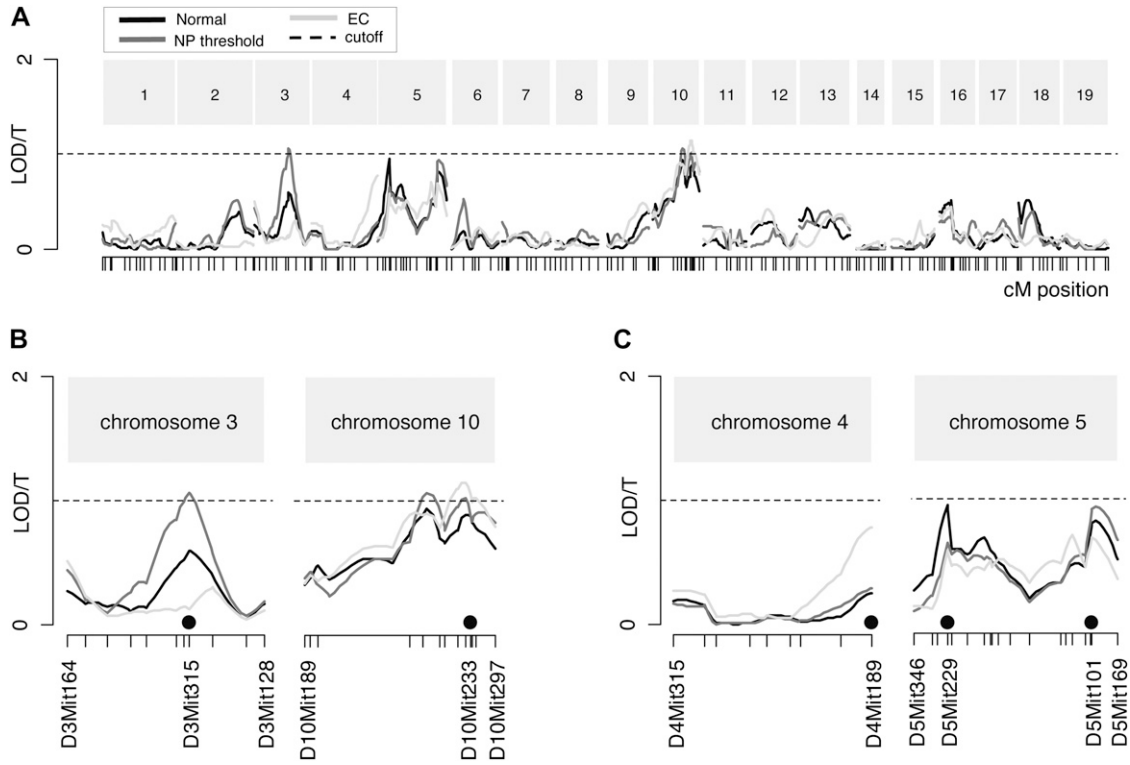

FIGURE 4.—Significant and suggestive modifier loci from genome-wide mapping. (A) Linkage data from two independent cohorts of AxB–*vb*/*vb* F_2 animals were pooled and analyzed for survival time as a quantitative trait by R/QTL under a normal model (solid line), by an extended Cox analysis for survival latency (lightly shaded line), or as a dichotomous trait under a nonparametric model (darkly shaded line). Results are plotted as the LOD score divided by the permutation-based threshold for each model. Secondary analyses with related analytical approaches showed similar results. (B) The nonparametric model detects significant linkage on chromosomes 3 and 10. The extended Cox model detects an overlapping linkage peak on chromosome 10, where the normal model is suggestive. (C) Additional suggestive linkages were seen on chromosomes 4 (extended Cox model) and 5 (normal QTL and dichotomous trait models). Solid circles indicate positions of the markers detailed in Figure 5.

logical barrier rather than manipulation of individual gene expression. Here, we have demonstrated modifier activity in the A/J background and identified two new modifier loci affecting the survival of *vibrator* mice. These loci appear to act through a bypass mechanism, distinct from the gene expression mechanism identified for the first modifier of *vibrator*, *Nxf1* (FLOYD *et al.* 2003), because the A/J background does not significantly alter

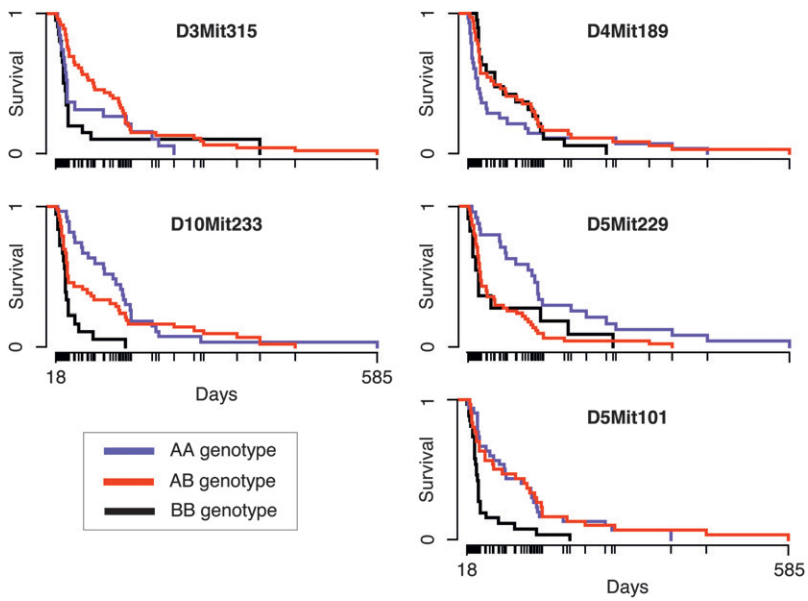

FIGURE 5.—Allele-specific effects and molecular heterosis. For marker loci at each significant (left) or suggestive (right) linkage peak, Kaplan–Meier plots for genotype-specific survival are shown. Results for D3Mit315 suggest molecular heterosis, with greater survival of heterozygotes than either homozygous phenotype. Results for D10Mit233 suggest a dominant or semidominant effect. Suggestive loci on chromosomes 4 and 5 are most consistent with simple dominance relationships. Tick marks at the bottom of each panel indicate timing of an individual event.

the level of PITPα nor the distribution of overt neuropathology within the discriminatory range of our assays. Indeed, compared with *Nxf1*^{CAST}-heterozygous *vibrators*, A/J *vibrators* show better survival despite greater neuropathology. We refer to the new modifier-of-*vibrator* loci reported here as *Mvb2* (chromosome 10) and *Mvb3* (chromosome 3). Our linkage data also provide suggestive evidence for linkage to a locus on chromosome 4 and two distinct loci on either end of chromosome 5. Because the mode of suppression appears to involve bypass of a requirement for high *Pitpna* expression, the A/J variants detected here may act on other mutations in PITP-dependent pathways.

We envision three classes of potential mechanisms for bypassing *vibrator* lethality: altered circuit robustness, altered vulnerability of discrete cell populations, and noncentral effects. A circuit robustness model implies that at least one specific neuronal ensemble that controls a vital function, compromised in *vibrator*, is more resistant to a similar level of neuropathology in one strain than in another. For example, a circuit with more redundancy in one component cell population might withstand a similar level of cellular damage simply by having more cells that can supply the same function. As with many neurodegenerative disorders, *vibrator* pathology shows selective vulnerability of some neuronal populations; an altered vulnerability model implies that at least one population is less vulnerable in the suppressed background. While the overall pattern of degeneration appears similar between *vibrator* animals on A/J and B6 backgrounds, we would not have adequate power in this sample size to detect subtle variations in frequency or moderate differences that are restricted to small numbers of cells in specific nuclei. Beyond neuropathology, loss of PITPα is known to affect a wide variety of non-neuronal cell types (Alb *et al.* 2003; Ile *et al.* 2006). Improved dietary metabolism or respiratory function, for example, may allow A/J *vibrators* to survive a higher degree of neuropathology. However, titration studies with an allelic series and selective transgene expression studies suggest that peripheral phenotypes of PITPα null animals are not present in *vb/vb* and that intestinal re-expression of PITPα is not sufficient to extend survival of otherwise null animals (Alb *et al.* 2007). Current evidence therefore suggests a central mechanism, although this has not been proved. We further recognize that these classes of mechanism are not mutually exclusive and, given that A/J-mediated survival of *vibrators* is multigenic, more than one mode of bypass may be relevant.

Genetic modifiers identified through activity on one gene of a pathway or network may often act on additional genes in the same pathway or on genes regulated through the same genetic mechanism (Moore *et al.* 1990; Blewitt *et al.* 2005; Concepcion *et al.* 2009). From this perspective, it will be of interest to determine whether the A/J background can suppress other PI-signaling mutants, such as *Inpp4a* (Nystuen *et al.* 2001), *Fig4* (Chow *et al.* 2007), and *Vac14* (Zhang *et al.* 2007; Jin *et al.* 2008), whose phenotypic similarities include tremor, premature lethality, degenerative pathology, and intracellular trafficking defects. Utilization of the captive variation in inbred strains in this way may provide tools for either broad or selective manipulation of physiological pathways.

The authors thank Bhavin Mehta and Peter Gent for assistance and Nicholas J. Schork for helpful discussions in the early phases of mapping. We thank the Moores University of California San Diego Cancer Center Histology Shared Resource for assistance with paraffin sections and standard histological stains. This work was supported by National Institutes of Health grant R01 GM086912 to B.A.H.

LITERATURE CITED

Alb, J. G., Jr., J. D. Cortese, S. E. Phillips, R. L. Albin, T. R. Nagy *et al.*, 2003 Mice lacking phosphatidylinositol transfer protein-alpha exhibit spinocerebellar degeneration, intestinal and hepatic steatosis, and hypoglycemia. J. Biol. Chem. **278:** 33501–33518.

Alb, J. G., Jr., S. E. Phillips, L. R. Wilfley, B. D. Philpot and V. A. Bankaitis, 2007 The pathologies associated with functional titration of phosphatidylinositol transfer protein alpha activity in mice. J. Lipid Res. **48:** 1857–1872.

Blewitt, M. E., N. K. Vickaryous, S. J. Hemley, A. Ashe, T. J. Bruxner *et al.*, 2005 An N-ethyl-N-nitrosourea screen for genes involved in variegation in the mouse. Proc. Natl. Acad. Sci. USA **102:** 7629–7634.

Broman, K. W., and S. Sen, 2009 *A Guide to QTL Mapping with R/qtl.* Springer, New York.

Broman, K. W., H. Wu, S. Sen and G. A. Churchill, 2003 R/qtl: QTL mapping in experimental crosses. Bioinformatics **19:** 889–890.

Chow, C. Y., Y. Zhang, J. J. Dowling, N. Jin, M. Adamska *et al.*, 2007 Mutation of FIG4 causes neurodegeneration in the pale tremor mouse and patients with CMT4J. Nature **448:** 68–72.

Cockcroft, S., and N. Carvou, 2007 Biochemical and biological functions of class I phosphatidylinositol transfer proteins. Biochim. Biophys. Acta **1771:** 677–691.

Concepcion, D., L. Flores-Garcia and B. A. Hamilton, 2009 Multipotent genetic suppression of retrotransposon-induced mutations by Nxf1 through fine-tuning of alternative splicing. PLoS Genet. **5:** e1000484.

de Vries, K. J., A. A. Heinrichs, E. Cunningham, F. Brunink, J. Westerman *et al.*, 1995 An isoform of the phosphatidylinositol-transfer protein transfers sphingomyelin and is associated with the Golgi system. Biochem. J. **310**(Pt. 2): 643–649.

Dietrich, W. F., J. Miller, R. Steen, M. A. Merchant, D. Damron-Boles *et al.*, 1996 A comprehensive genetic map of the mouse genome. Nature **380:** 149–152.

Floyd, J. A., D. A. Gold, D. Concepcion, T. H. Poon, X. Wang *et al.*, 2003 A natural allele of Nxf1 suppresses retrovirus insertional mutations. Nat. Genet. **35:** 221–228.

Hamilton, B. A., D. J. Smith, K. L. Mueller, A. W. Kerrebrock, R. T. Bronson *et al.*, 1997 The vibrator mutation causes neurodegeneration via reduced expression of PITP alpha: positional complementation cloning and extragenic suppression. Neuron **18:** 711–722.

Helmkamp, G. M., Jr., M. S. Harvey, K. W. Wirtz and L. L. Van Deenen, 1974 Phospholipid exchange between membranes. Purification of bovine brain proteins that preferentially catalyze the transfer of phosphatidylinositol. J. Biol. Chem. **249:** 6382–6389.

Ile, K. E., G. Schaaf and V. A. Bankaitis, 2006 Phosphatidylinositol transfer proteins and cellular nanoreactors for lipid signaling. Nat. Chem. Biol. **2:** 576–583.

Jin, N., C. Y. Chow, L. Liu, S. N. Zolov, R. Bronson *et al.*, 2008 VAC14 nucleates a protein complex essential for the acute interconversion of PI3P and PI(3,5)P(2) in yeast and mouse. EMBO J. **27:** 3221–3234.

Johannes, F., 2007 Mapping temporally varying quantitative trait loci in time-to-failure experiments. Genetics **175:** 855–865.

McMurray, W. C., and R. M. Dawson, 1969 Phospholipid exchange reactions within the liver cell. Biochem. J. **112:** 91–108.

Moore, K. J., D. A. Swing, N. G. Copeland and N. A. Jenkins, 1990 Interaction of the murine dilute suppressor gene (*dsu*) with fourteen coat color mutations. Genetics **125:** 421–430.

Nystuen, A., M. E. Legare, L. D. Shultz and W. N. Frankel, 2001 A null mutation in inositol polyphosphate 4-phosphatase type I causes selective neuronal loss in weeble mutant mice. Neuron **32:** 203–212.

Offermanns, S., K. Hashimoto, M. Watanabe, W. Sun, H. Kurihara *et al.*, 1997a Impaired motor coordination and persistent multiple climbing fiber innervation of cerebellar Purkinje cells in mice lacking Galphaq. Proc. Natl. Acad. Sci. USA **94:** 14089–14094.

Offermanns, S., C. F. Toombs, Y. H. Hu and M. I. Simon, 1997b Defective platelet activation in G alpha(q)-deficient mice. Nature **389:** 183–186.

Phillips, S. E., K. E. Ile, M. Boukhelifa, R. P. Huijbregts and V. A. Bankaitis, 2006a Specific and nonspecific membrane-binding determinants cooperate in targeting phosphatidylinositol transfer protein beta-isoform to the mammalian trans-Golgi network. Mol. Biol. Cell **17:** 2498–2512.

Phillips, S. E., P. Vincent, K. E. Rizzieri, G. Schaaf, V. A. Bankaitis *et al.*, 2006b The diverse biological functions of phosphatidylinositol transfer proteins in eukaryotes. Crit. Rev. Biochem. Mol. Biol. **41:** 21–49.

Pletcher, M. T., P. McClurg, S. Batalov, A. I. Su, S. W. Barnes *et al.*, 2004 Use of a dense single nucleotide polymorphism map for in silico mapping in the mouse. PLoS Biol. **2:** e393.

Weimar, W. R., P. W. Lane and R. L. Sidman, 1982 *Vibrator* (*vb*): a spinocerebellar system degeneration with autosomal recessive inheritance in mice. Brain Res. **251:** 357–364.

Zhang, Y., S. N. Zolov, C. Y. Chow, S. G. Slutsky, S. C. Richardson *et al.*, 2007 Loss of Vac14, a regulator of the signaling lipid phosphatidylinositol 3,5-bisphosphate, results in neurodegeneration in mice. Proc. Natl. Acad. Sci. USA **104:** 17518–17523.

Communicating editor: D. W. Threadgill

GENETICS

Supporting Information
http://www.genetics.org/cgi/content/full/genetics.110.125906/DC1

Modifier Genes for Mouse Phosphatidylinositol Transfer Protein α (*vibrator*) That Bypass Juvenile Lethality

Dorothy Concepcion, Frank Johannes, Yuan Hung Lo, Jay Yao, Jerry Fong* and Bruce A. Hamilton

DOI: 10.1534/genetics.110.125906

Files S1 and S2

Supporting Movie and Supporting Data

Files S1 and S2 are available for download at http://www.genetics.org/cgi/content/full/genetics.110.125906/DC1.

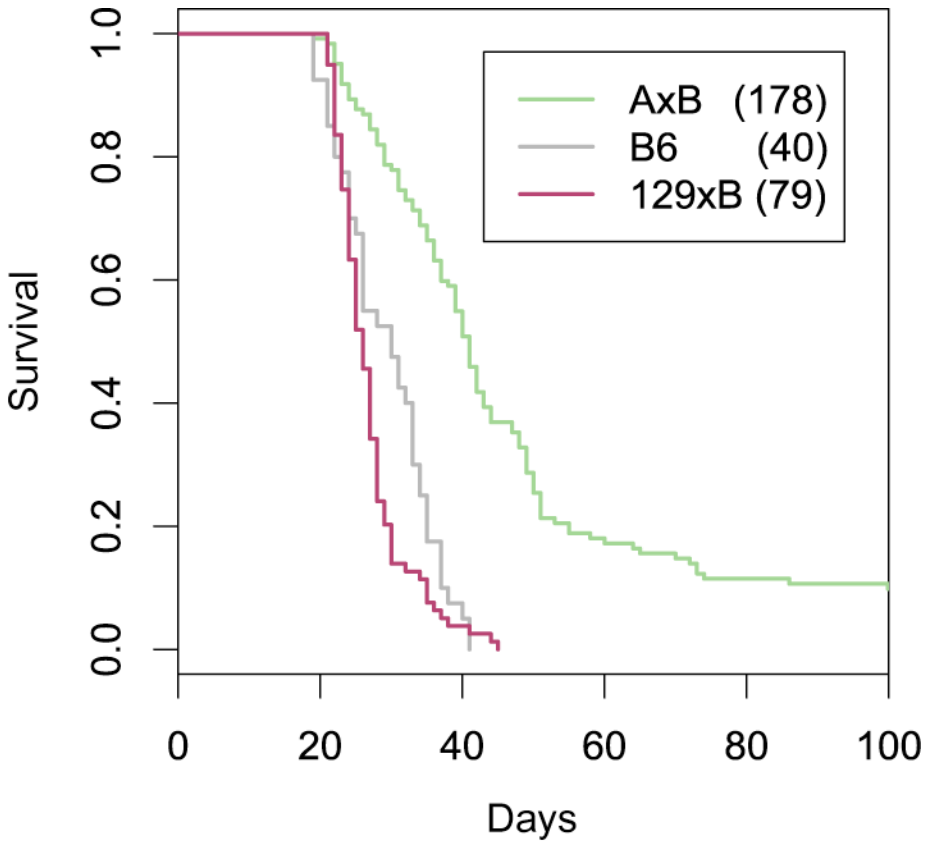

FIGURE S1.—Lack of modifier activity in 129S1/SvImJ. Kaplan-Meier plots of 79 129S1 x B6–*vb* F2 *vb/vb* animals shows no evidence for suppressor activity predicted from the (129xB6)–*Gnaq* x B6–*vb* cross described in text. AxB and B6 *vb/vb* cohorts are those described in the main text and shown in Figure 1. The modest difference between 129xB and B6 *vb/vb* cohorts falls just short conventional thresholds for nominal significance (P=0.06), but in the direction of *vb*-sensitizing 129S1 alleles.

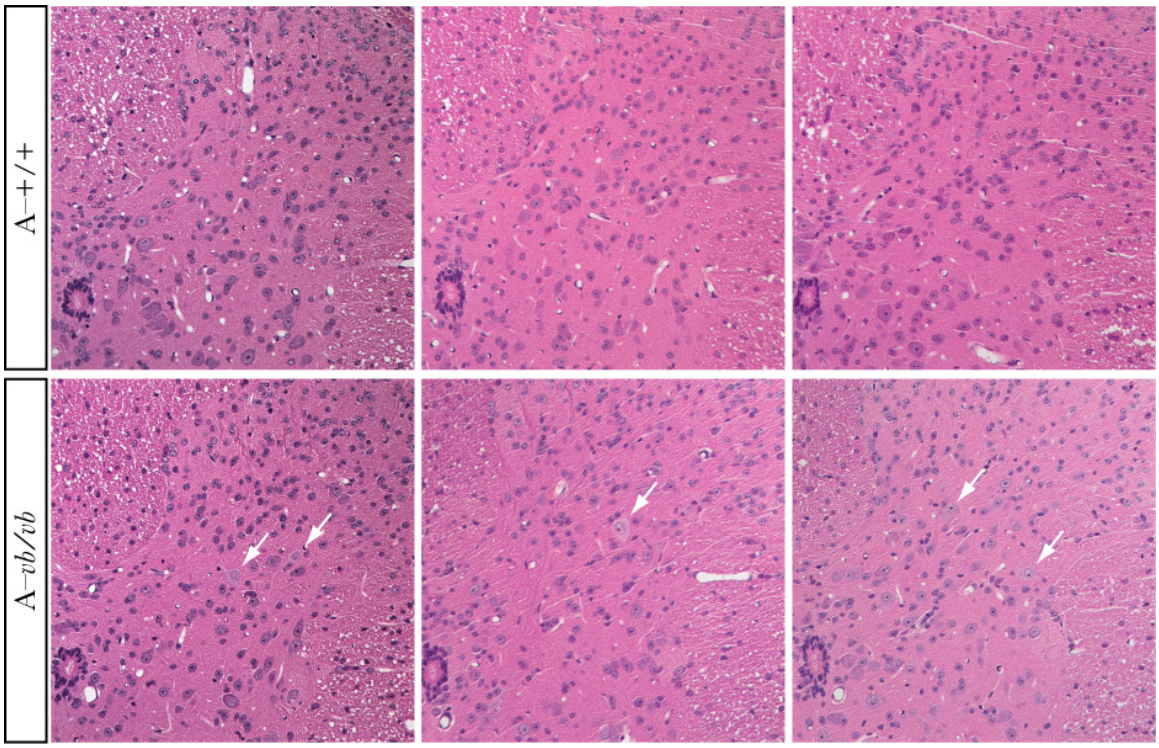

FIGURE S2.—Faint staining cells in A–*vb*. Non-adjacent sections from *vibrator* and littermate +/+ control thoracic spinal cords show faint staining cells with variable degrees of swelling (white arrows), consistent with cells reported in HAMILTON ET AL., 1997 and FLOYD ET AL, 2003. Images are oriented with dorsal up and the central canal visible at bottom left of each panel.

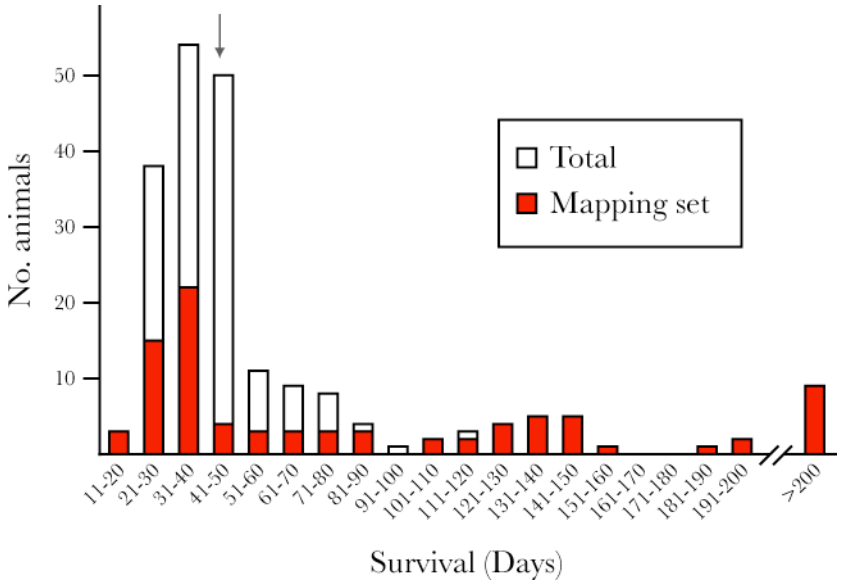

FIGURE S3.—Distribution of A x B *vibrator* survival. Data are grouped into 10-day bins for representation in the histogram. Red bars indicate number of animals in the mapping panel for each bin, white bars indicate the total number of animals observed in that bin. The 41-50 day bin excludes the range 42-48 d from the mapping set; grey arrow indicates maximum lifespan among B6–*vb*/*vb*.